International Journal of Information, Control and Computer Sciences
ISSN: 2517-9942
Vol:9, No:2, 2015

Study of Natural Patterns on Digital Image Correlation Using Simulation Method

Gang Li, Ghulam Mubashar Hassan, Arcady Dyskin, Cara MacNish

***Abstract*—**Digital image correlation (DIC) is a contactless full-field displacement and strain reconstruction technique commonly used in the field of experimental mechanics. Comparing with physical measuring devices, such as strain gauges, which only provide very restricted coverage and are expensive to deploy widely, the DIC technique provides the result with full-field coverage and relative high accuracy using an inexpensive and simple experimental setup. It is very important to study the natural patterns effect on the DIC technique because the preparation of the artificial patterns is time consuming and hectic process. The objective of this research is to study the effect of using images having natural pattern on the performance of DIC. A systematical simulation method is used to build simulated deformed images used in DIC. A parameter (subset size) used in DIC can have an effect on the processing and accuracy of DIC and even cause DIC to failure. Regarding to the picture parameters (correlation coefficient), the higher similarity of two subset can lead the DIC process to fail and make the result more inaccurate. The pictures with good and bad quality for DIC methods have been presented and more importantly, it is a systematic way to evaluate the quality of the picture with natural patterns before they install the measurement devices.

***Keywords*—**Digital image correlation (DIC), Deformation simulation, Natural pattern, Subset size.

I. Introduction

DIGITAL image correlation (DIC) is a contactless full-field displacement and strain measurement technique commonly used in the field of experimental mechanics. It can provide the full-fields displacement and strains with sub-pixel accuracy by using the digital images of the specimen's surface obtained before and after deformation. It was first developed in 1980s [1] and now has been increasing in popularity, especially in micro- and nano-scale mechanical testing applications due to its relative ease of implementation and use. The DIC technique has been applied in the many areas such as determining the deformation field and the characteristics of the various materials subjected to various loading conditions [2], identification of the mechanical parameters of a particular material including Young's modulus, Poisson's ratio [3], stress intensity factor [4] and residual stress [5],validation of computational models such as the FEM models [6].

Gang Li and Ghulam Mubashar are with the University of Western Australia, Australia (e-mail: 21189402@student.uwa.edu.au, ghulam.hassan@research.uwa.edu.au).

Arcady Dyskin is Winthrop Professor with the School of Civil & Resource Engineering, University of Western Australia, Australia (e-mail: arcady.dyskin@uwa.edu.au).

Cara MacNish is Professor with School of Computer Science & Software Engineering, University of Western Australia, Australia (e-mail: cara.macnish@uwa.edu.au)

The digital images used in DIC are the specimen surface represented by the gray intensity distribution. Two types of situations arise in practice. First, the natural texture of the specimen surface has its own gray intensity distribution. Some of them are sufficient to use the correlation algorithm directly. The displacement field measurement used compressed mineral wool samples with no special preparation [7] which means the natural pattern was directly used in that experiment. Then another way to get a random gray intensity distribution is artificially made by spraying black and/or white paints, or other techniques [1]. In both situations, it is essential to evaluate the quality of the texture when DIC is applied and assess the displacements and strains uncertainties as well.

In general, the quality of the natural texture can be described as roughness, adhesiveness, sharpness and hardness. One advantage of using natural patterns is to simplify the specimen preparation for the industrial application because the artificial speckle patterns used in the test are not applicable in real world. Another reason is surface preparation is found to be of minimal importance under high magnification. The natural surface topography is sufficient for microscopic measurements using proper illumination of the surface. White light illumination should be used with an adjustment of the angle of incidence to generate a surface with a large range in gray-scale intensity [8].

Therefore, the study of the natural patterns for the DIC technique is essential and helpful for the future industrial applications. In this article, an investigation of the effects for natural patterns is done by the simulation results using computer programs.

II. Problem Identification

The texture in image analysis could be defined as the natural pattern to characterize objects [9]. Over the past years, researchers have investigated the image textures and their effects on measurement accuracy [10]. Also the uncertainty analysis of the different textures has been done to evaluate the quality of the image texture [11]. Whether the texture is good or bad can be very critical for DIC method. For example, bad texture such as a uniformly colored image can lead to failure of DIC.

Generally, there are some aspects to define the quality of the textures such as the brightness, shape, color. In the numerical models, the gray level intensity distribution is used to describe the image textures in black and white photographs. As the uniform distribution can be simply very bad for correlation, the pictures with varied distribution will be investigated. Also natural textures can be very different

because of different objects captured, light environments and capture devices.

The quality of the pattern is firstly introduced on the study of artificial speckle pattern on the specimen surface. Different parameters, such as mean speckle size [12], subset entropy [13] and sum of square of subset intensity gradients (SSSIG) [14] have been proposed to evaluate the quality of the speckle pattern. Furthermore, the pattern of the image directly affects the selection of subset size. For some speckle patterns a large subset must be chosen to provide a reliable result, while for some speckle patterns with sharp contrast, a very small subset containing sufficiently distinctive intensity pattern yields a satisfactory result.

Regarding to the natural textures, two criteria were proposed from a texture study [11] to evaluate the best compromise between measurement uncertainty and spatial resolution prior to any mechanical test.

This article aims at improving the understanding of the digital image correlation regarding the natural textures and investigating the characteristics to determine the quality of the image textures which affect the accuracy of the result.

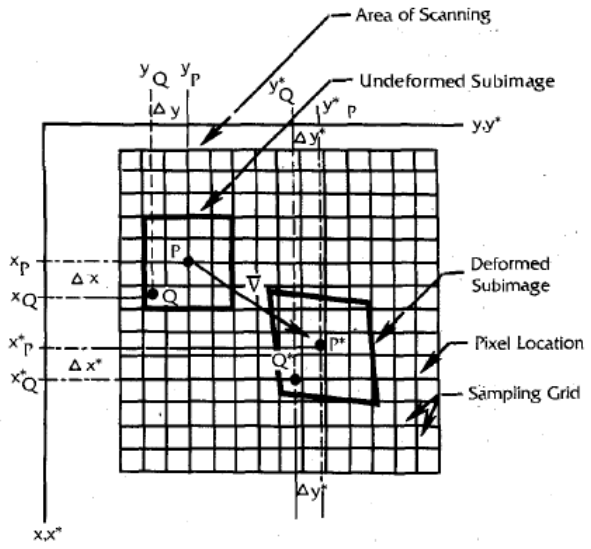

Fig. 1 Deformation of a sub-image in a sampling grid [1]

III. Theory

A. The Method of Digital Image Correlation

Cross-correlation method is widely used to describe the correlation of two functions by using the value of the correlation coefficient. The larger correlation coefficient is, the more similar the two functions are. The method of DIC is based on the application of cross-correlation method to compare digital images. After obtaining the digital images of the specimen surface before and after deformation, the DIC can compute the motion of each image pixel by comparing the deformed image and reference image.

In DIC, the region of interest (ROI) should be firstly defined or specified in the referenced image. As shown in Fig. 1, the basic principle of DIC is to track the same points (P and Q) in the deformed and referenced images. Since the first-order shape function allows translation, rotation, shear, normal strains and their combinations of the subset, it is the most commonly used.

For the subset center point $P(x_0, y_0)$ in the reference image corresponding to $P^*(x_0^*, y_0^*)$ in the deformed image, the point $Q(x_i, y_i)$ can be corresponded to point $Q^*(x_i^*, y_i^*)$

$$x_i^* = x_i + u + \frac{\partial u}{\partial x}\Delta x + \frac{\partial u}{\partial y}\Delta y \quad (1)$$

$$y_i^* = y_i + v + \frac{\partial v}{\partial x}\Delta x + \frac{\partial v}{\partial y}\Delta y \quad (2)$$

where u and v are the displacements for the subset centers in the x and y directions respectively. The terms Δx and Δy are the distances from the subset center to point P(x, y) which can be described as

$$\Delta x = x_i - x_0 \quad \Delta y = y_i - y_0 \quad (3)$$

In the DIC computation process, the intensity values of the image are used for correlation. The value of each pixel is typically an eight-bit number (ranges in value from 0 to 255) with the lowest value representing black, highest value white, and values in between representing different shades of gray. In order to build the correlation using the intensity value of the image, a typical correlation function which measures how well subsets match is given as:

$$S = \left(x, y, u, v, \frac{\partial u}{\partial x}, \frac{\partial u}{\partial y}, \frac{\partial v}{\partial x}, \frac{\partial v}{\partial y}\right) = \frac{\sum[F(x,y) * G(x^*, y^*)]}{[\sum(F(x,y)^2) * \sum(G(x^*, y^*)^2)]^{\frac{1}{2}}} \quad (4)$$

where F(x, y) is the intensity value at coordinate (x, y) and $G(x^*, y^*)$ is t the intensity value at point (x^*, y^*) of the deformed image.

Image correlation is to determine values for $u, v, \frac{\partial u}{\partial x}, \frac{\partial u}{\partial y}, \frac{\partial v}{\partial x}$, and $\frac{\partial v}{\partial y}$ which can maximize the correlation coefficient (S).

Points in the deformed subset may locate between pixels. Before correlate the deformed and referenced images, the intensity of these points with sub-pixel locations must be provided. Thus, a suitable interpolation scheme should be utilized. Currently various sub-pixel interpolation schemes including bilinear interpolation, bicubic interpolation, bicubic B-spline interpolation, biquintic B-spline interpolation and bicubic spline interpolation have been used. It can be seen that a high-order interpolation scheme is highly recommended [15] since it provides higher accuracy and better convergence. Therefore, the bicubic spline interpolation scheme is used in the simulation process.

As stated before, image correlation is to find the six deformation parameters, $u, v, \frac{\partial u}{\partial x}, \frac{\partial u}{\partial y}, \frac{\partial v}{\partial x}, and$ $\frac{\partial v}{\partial y}$ which can maximize the correlation function. In order to obtain these parameters, the iteration method such as Newton-Raphson method proposed to be used in DIC [16].

The Newton-Raphson method is based on the calculation of correction terms which improve initial guesses. The correction

formula is:

$$\Delta P_i = -H^{-1}(Pi) * \nabla(P_i) \quad (5)$$

where

$$P_i = \begin{Bmatrix} u \\ v \\ \frac{\partial u}{\partial x} \\ \frac{\partial u}{\partial y} \\ \frac{\partial v}{\partial x} \\ \frac{\partial v}{\partial y} \end{Bmatrix} \quad (6)$$

Pi is the matrix of the six deformation parameters. $\nabla(P_i)$ is the Jacobian matrix. Each term in the Jacobian is the derivative of the correlation function evaluated at guess i. The Jacobian matrix is

$$\nabla(P_i) = \begin{Bmatrix} \frac{\partial S}{\partial u} \\ \frac{\partial S}{\partial v} \\ \frac{\partial S}{\partial(\frac{\partial u}{\partial x})} \\ \frac{\partial S}{\partial(\frac{\partial u}{\partial y})} \\ \frac{\partial S}{\partial(\frac{\partial v}{\partial x})} \\ \frac{\partial S}{\partial(\frac{\partial v}{\partial y})} \end{Bmatrix} \quad (7)$$

H (Pi) is the Hessian Matrix which consists of the send derivatives of the correlation function.

$$H(P_i) = \begin{Bmatrix} \frac{\partial^2 S}{\partial u \partial u} & \frac{\partial^2 S}{\partial u \partial v} & \frac{\partial^2 S}{\partial u \partial(\frac{\partial u}{\partial x})} & \frac{\partial^2 S}{\partial u \partial(\frac{\partial u}{\partial y})} & \frac{\partial^2 S}{\partial u \partial(\frac{\partial v}{\partial x})} & \frac{\partial^2 S}{\partial u \partial(\frac{\partial v}{\partial y})} \\ \frac{\partial^2 S}{\partial v \partial u} & \frac{\partial^2 S}{\partial v \partial v} & \frac{\partial^2 S}{\partial v \partial(\frac{\partial u}{\partial x})} & \frac{\partial^2 S}{\partial v \partial(\frac{\partial u}{\partial y})} & \frac{\partial^2 S}{\partial v \partial(\frac{\partial v}{\partial x})} & \frac{\partial^2 S}{\partial v \partial(\frac{\partial v}{\partial y})} \\ \frac{\partial^2 S}{\partial(\frac{\partial u}{\partial x})\partial u} & \frac{\partial^2 S}{\partial(\frac{\partial u}{\partial x})\partial v} & \frac{\partial^2 S}{\partial(\frac{\partial u}{\partial x})\partial(\frac{\partial u}{\partial x})} & \frac{\partial^2 S}{\partial(\frac{\partial u}{\partial x})\partial(\frac{\partial u}{\partial y})} & \frac{\partial^2 S}{\partial(\frac{\partial u}{\partial x})\partial(\frac{\partial v}{\partial x})} & \frac{\partial^2 S}{\partial(\frac{\partial u}{\partial x})\partial(\frac{\partial v}{\partial y})} \\ \frac{\partial^2 S}{\partial(\frac{\partial v}{\partial x})\partial u} & \frac{\partial^2 S}{\partial(\frac{\partial v}{\partial x})\partial v} & \frac{\partial^2 S}{\partial(\frac{\partial v}{\partial x})\partial(\frac{\partial u}{\partial x})} & \frac{\partial^2 S}{\partial(\frac{\partial v}{\partial x})\partial(\frac{\partial u}{\partial y})} & \frac{\partial^2 S}{\partial(\frac{\partial v}{\partial x})\partial(\frac{\partial v}{\partial x})} & \frac{\partial^2 S}{\partial(\frac{\partial v}{\partial x})\partial(\frac{\partial v}{\partial y})} \\ \frac{\partial^2 S}{\partial(\frac{\partial u}{\partial y})\partial u} & \frac{\partial^2 S}{\partial(\frac{\partial u}{\partial y})\partial v} & \frac{\partial^2 S}{\partial(\frac{\partial u}{\partial y})\partial(\frac{\partial u}{\partial x})} & \frac{\partial^2 S}{\partial(\frac{\partial u}{\partial y})\partial(\frac{\partial u}{\partial y})} & \frac{\partial^2 S}{\partial(\frac{\partial u}{\partial y})\partial(\frac{\partial v}{\partial x})} & \frac{\partial^2 S}{\partial(\frac{\partial u}{\partial y})\partial(\frac{\partial v}{\partial y})} \\ \frac{\partial^2 S}{\partial(\frac{\partial v}{\partial y})\partial u} & \frac{\partial^2 S}{\partial(\frac{\partial v}{\partial y})\partial v} & \frac{\partial^2 S}{\partial(\frac{\partial v}{\partial y})\partial(\frac{\partial u}{\partial x})} & \frac{\partial^2 S}{\partial(\frac{\partial v}{\partial y})\partial(\frac{\partial u}{\partial y})} & \frac{\partial^2 S}{\partial(\frac{\partial v}{\partial y})\partial(\frac{\partial v}{\partial x})} & \frac{\partial^2 S}{\partial(\frac{\partial v}{\partial y})\partial(\frac{\partial v}{\partial y})} \end{Bmatrix} \quad (8)$$

The Newton-Raphson method is implemented by first obtaining an initial estimate for the six deformation parameters. The partial corrections are calculated using iteration formula. These corrections are added to the initial guess and the process is iterated until convergence is obtained.

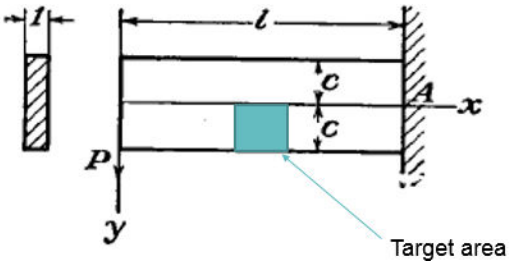

Fig. 2 Theoretical displacements scenario

B. Theoretical Displacements Calculation

In order to make the deformation simulation, the theoretical displacements need to be obtained at first. The scenario is presumed in the project as shown in Fig. 2 [17]. The target area is in the middle of the cantilever beam and the force is applied on the left side of the beam.

All the parameters are set reasonably. The material of the beam is aluminum with Young's Modulus (E=69GPa), Poisson's ratio (v=0.334) and Shear Modulus (G=26GPa). The dimension of the beam is L=0.5m, c=0.1m and moment of inertia is I= 1.67 cm^4. The value of the force is P=500N.

The displacements formulas are [17]:

$$u = -\frac{Px^2y}{2EI} - \frac{vPy^3}{6EI} + \frac{Py^3}{6IG} + \left(\frac{PL^2}{2EI} - \frac{Pc^2}{2IG}\right)y \quad (9)$$

$$v = \frac{vPxy^2}{2EI} + \frac{Px^3}{6EI} - \frac{PL^2x}{2EI} + \frac{PL^3}{3EI} \quad (10)$$

The target area is represented by an image of 250×250 pixels. In using the formulas, each point of the target area could have its own horizon and vertical displacement. As a result, the full-field horizontal and vertical displacement could be obtained after calculating all the pixels of the image.

After input all the process into the MATLAB, we can easily obtain the full-field theoretical displacements (horizontal and vertical) for the target area as shown in Fig 3.

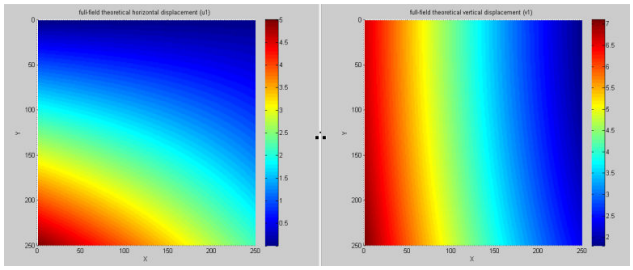

Fig. 3 Full-field theoretical horizontal and vertical displacement

C. Deformation Simulation Method

Deformation simulation method is to simulate the theoretical displacements on the referenced image in order to make the simulated deformed image. Due to the computation capability, the accuracy level we can achieve is 0.1 pixels. The referenced image is initially enlarged 10 times using the bicubic interpolation. As a result, the original referenced image is converted to the size of 2500×2500 pixels from 250×250 pixels size. Each point becomes one 10×10 subsets.

Simultaneously, the theoretical displacements are rounded off to 0.1 pixels accuracy level. The new position of each 10×10 subset is

$$X_i = X_0 + u_i \quad (11)$$
$$Y_i = Y_0 + v_i \quad (12)$$

Subsets may overlap each other or have some space between two subsets because of the variation of the displacements. We take the average values of the intensity values when they have the overlaps. For the subsets which have some space, we take the average values of intensity values near the space.

At this moment, we have successfully applied the theoretical displacement on the enlarged reference image. Then the deformed image is decreased to the original size using the same method as it is magnified. The simulated deformed image finally is obtained as shown in Fig. 4.

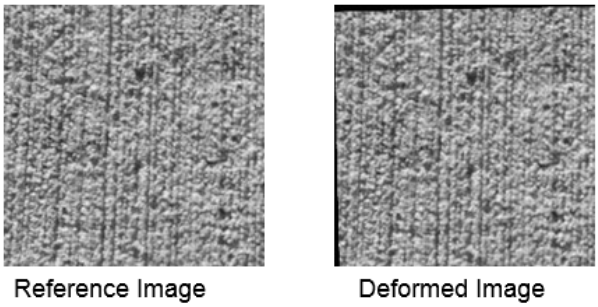

Fig. 4 Deformation simulation results

IV. Methodology

The approach used to study the effect of natural patterns is shown in Fig. 5.

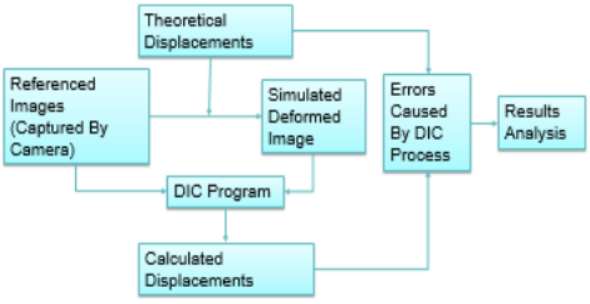

Fig. 5 Schematic illustration of the methodology

In order to analyze the effect of parameters using natural textures on the results of the digital image correlation method, the first thing to do is to capture the textures on the surfaces of the objects. At this stage, the photographs of different textures will be captured as the sources of the analysis. Twenty pictures are captured and there are three pictures which contain fractures and four pictures which are out of focus. As a result, thirteen pictures have been analyzed as the referenced images in our study as shown in Fig. 6.

Fig. 6 Sample pictures captured by camera

After obtaining the theoretical displacements, we use the deformation simulation method and get the simulated deformed image. Then the DIC program has been implemented to get the calculated horizontal and vertical displacements using the referenced images and deformed images.

After comparing the calculated displacements with the theoretical displacements, the errors of horizontal and vertical displacements caused by the DIC process have been obtained. The total error is:

$$e = \sqrt{{e_x}^2 + {e_y}^2} \quad (13)$$

All the errors used in the discussions are the total errors.

V. Results and Discussions

A. DIC Program Failure Conditions

In this study, the DIC can sometimes fail due to reasons, such as, not suitable natural pattern and small size of the subset. The reason is either natural pattern does not have enough intensity variation or subset size is too small to have intensity variation which makes difficult for DIC to correlate subsets from the reference and deformed images.

In order to study the effect of subset size, the subset size of 21 x 21 pixels is firstly used for the pattern shown in Fig. 7. The maximum error is found to be around 0.08 pixels and the mean error is found to be around 0.0309 pixels.

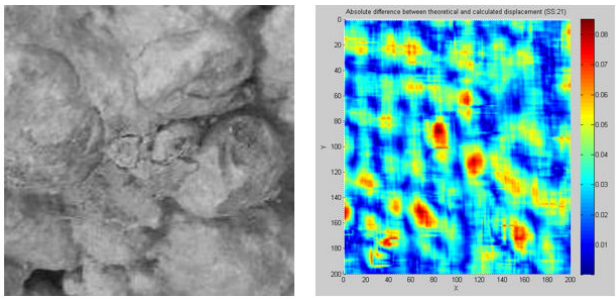

Fig. 7 The errors using subset size of 21 pixels with the natural pattern T5

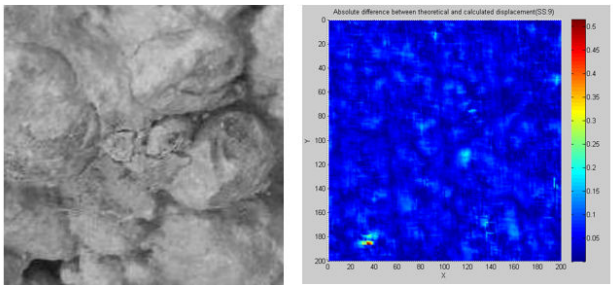

Fig. 8 The errors using subset size of 9 pixels with the natural pattern T5

Afterwards, the subset size is decreased from 21 x 21 pixels to 9 x 9 pixels and the results are shown in Fig. 8. The maximum error is around 0.5 pixels and it is located in a particular area of the left bottom corner. However, the mean error is around 0.0476 pixels. Therefore, most of the pixels of the reference images are found in deformed image except the area with the higher error. It can be observed that the error is correlated to the black hole in the reference image. The variation of intensity value in that area is lower than rest of the image which results in making it difficult for DIC to find displacement of pixels in that area with high accuracy.

All natural patterns are analyzed with both subset sizes of 21 x 21 pixels and 9 x 9 pixels. The results are summarized in Table I.

TABLE I
RESULTS FOR ALL PATTERNS USING SUBSET SIZES OF 21 PIXELS AND 9 PIXELS

No. of natural pattern	Subset size (21 pixels)			Subset size (9 pixels)			Z=R9/R21	DIC failure
	Max Error	Mean Error	R21(Max over mean)	Max Error	Mean Error	R9(Max over mean)		
T1	0.05	0.025	1.976	0.11	0.0342	3.216	1.62	No
T5	0.08	0.030	2.589	0.5	0.0476	10.504	4.05	Yes
T6	0.1	0.048	2.057	0.45	0.064	6.944	3.37	Yes
T9	0.16	0.076	2.099	0.3	0.0958	3.131	1.49	No
T11	0.1	0.047	2.123	0.2	0.062	3.225	1.51	No
T12	0.11	0.051	2.156	0.25	0.0646	3.870	1.79	No
T14	0.12	0.060	1.973	0.25	0.0772	3.238	1.64	No
T15	0.1	0.049	2.020	0.25	0.0644	3.882	1.92	No
T16	0.07	0.034	2.029	0.13	0.0454	2.863	1.41	No
T17	0.11	0.051	2.123	0.25	0.0665	3.759	1.77	No
T18	0.12	0.053	2.238	0.22	0.0685	3.211	1.43	No
T19	0.18	0.061	2.922	1.03	0.0819	12.576	4.30	Yes
T20	0.14	0.066	2.092	0.25	0.0849	2.944	1.40	No

Regarding the subset size of 21 x 21 pixels, the ratios of maximum error over mean error (R21) are around 2 except for pattern T5 and T19 which are 2.589 and 2.9221 respectively. Thus these two patterns don't cause the DIC program to fail. Similarly, for the subset size of 9 x 9 pixels, the ratios of maximum error over mean error (R9) are around 3 except for T5, T6 and T19 which are 10.504, 6.944 and 12.576. We introduce the parameter Z to describe whether the smaller subset leads to failure or not.

$$Z = \frac{R_9}{R_{21}} \tag{14}$$

The values of parameter Z are mostly in the range of 1.4 to 2 except for pattern T5, T6 and T19 which exceeded the range and are 4.05, 3.37 and 4.30 respectively. Thus, the subset size of 9 x 9 pixels causes the DIC program to fail in pattern T5, T6 and T19.

B. Subset Size Effect

TABLE II
MEAN ERRORS WITH DIFFERENT SUBSET SIZE REGARDING TO PATTERN T1

Subset size (pixels)	Mean error
9 x 9	0.0342
11 x 11	0.032
13 x 13	0.0304
15 x 15	0.0290
17 x 17	0.0278
19 x 19	0.0265
21 x 21	0.0253
31 x 31	0.0187
41 x 41	0.0126
61 x 61	0.0105
81 x 81	0.0173
101 x 101	0.0267

Subset size is a critical parameter in the study of the accuracy. In order to analyze the effect of subset size on the accuracy of DIC, different subset sizes are used to the natural pattern T1. The results are tabulated in Table II.

The graph plotted for the mean errors with respect to different subset sizes is presented in Fig. 9.

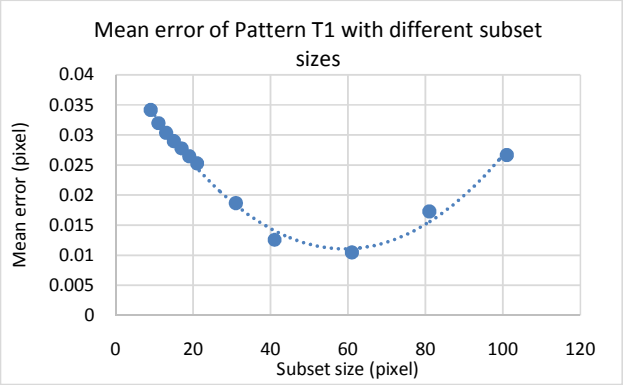

Fig. 9 Mean errors with different subset sizes (Pattern T1)

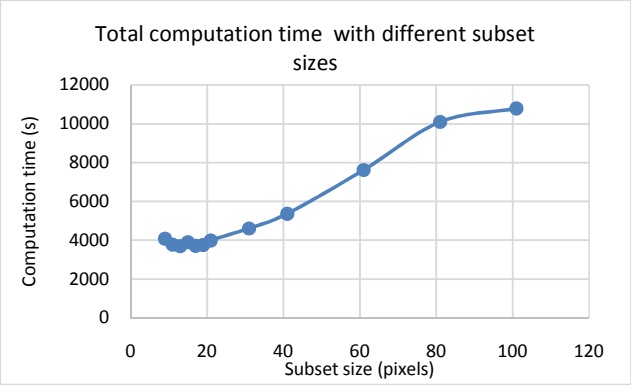

Fig. 10 Total computation time with different subset sizes

From the graph, it can be observed that the suitable subset size is 61 x 61 pixels which provide highest accuracy having 0.01 pixels of mean error. For subset sizes smaller than 61 x 61 pixels, the mean errors decrease with the increase in the subset size. After achieving the highest accuracy for subset size of 61 x 61 pixels, the mean errors increase with the increase in the subset size. Furthermore, larger subset sizes also cause the computation time to increase. The computation time includes time of spline process and time of optimization process. Considering the effect of subset size on the computation time, the results are tabulated in Table III.

TABLE III
COMPUTATION TIME AND ITERATION TIMES WITH DIFFERENT SUBSET SIZES

Subset size (pixels)	Time of spline (s)	Time of optimization (s)	Total computation time (s)	average iteration times
9 x 9	2042.1	2041	4083.3	8.06
11 x 11	1888.37	1890	3776	7.57
13 x 13	1848.85	1848	3697	7.32
15 x 15	1955	1950	3907.4	7.18
17 x 17	1855.97	1860	3711.2	7.1
19 x 19	1880	1880	3765	7.03
21 x 21	1997.5	1994	3991.4	6.98
31 x 31	2306.1	2300	4610.8	6.2
41 x 41	2684.1	2680	5367.5	5.5
61 x 61	3810.7	3810	7619	4.07
81 x 81	5048.6	5050	10096.8	3.07
101 x 101	5396.85	5400	10793.3	2.18

Consequently, the graphs of computation time and iteration times are plotted as shown in Figs. 10 and 11 respectively.

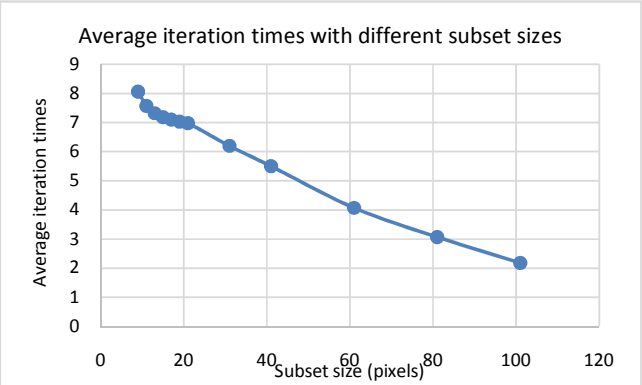

Fig. 11 Average iteration times with different subset sizes

Regarding to the computation times, it fluctuates from subset size of 9 x 9 pixels to 21 x 21 pixels with the range of around 3700s to 4000s. However after subset size of 21 x 21 pixels, the computation time increases significantly with the increase of the subset size. This causes the negative effect on the efficiency of DIC. For the iteration times, it can be observed clearly that higher subset sizes results in the lower iterations. Thus, it is possible that the smaller subset size may leads to failure of DIC because number of iteration exceeds the iterations limit for optimization in the DIC technique.

Conclusively, due to the effect of the subset size, it is better to choose the suitable subset size according to the required accuracy and efficiency. For instance, consider pattern T1, if high accuracy is required then subset size of 61 x 61 pixels should be used to obtain the accuracy level of 0.01 pixels. However, if the application requires accuracy level of 0.03 pixels, then optimal subset size is 17 x 17 pixels. Therefore, it is important that the subset size is chosen in accordance with the expected error acceptance criterion.

C. Correlation Coefficient Effect

Regarding to the correlation coefficient distribution, each point of the image has its own correlation coefficient based on the subset size used in the program. The correlation coefficient distribution with its referenced image is shown in Fig. 12.

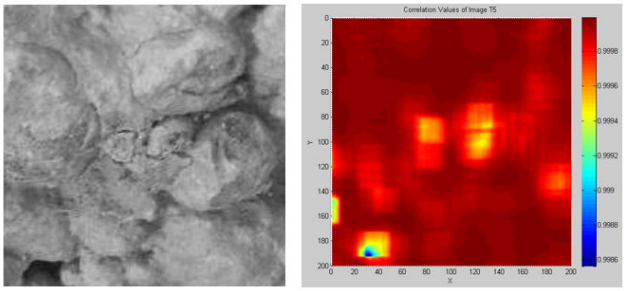

Fig. 12 Correlation coefficient distribution of pattern T5

From the distribution, the lowest value occurs in the left bottom corner of the image which is the correlation of pixels in the black part of the image. Based on the correlation function, the variation in the intensity levels in the subset provides a better result. The area of the pattern where the intensity variation does not exist significantly then correlation is lower. For the analysis of correlation effect on the image pattern, the correlation coefficient distribution of another pattern T6 is shown in Fig. 13. The areas with lower variation of intensity values had low correlation values compared to other areas.

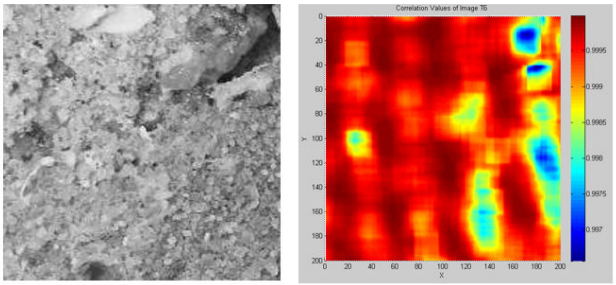

Fig. 13 Correlation coefficient distribution of pattern T6

Considering the quality of the natural patterns, a parameter is introduced which provides the minimum value of correlation coefficient to estimate the quality of the patterns.

In order to build the relationship between the minimum value of correlation coefficient and the quality of the patterns, the minimum correlation coefficient values from different patterns with different mean errors are presented in Table IV.

TABLE IV
MINIMUM CORRELATION COEFFICIENT OF DIFFERENT PATTERNS

No. of Pattern	Maximum error	Mean error	min correlation coefficient
T1	0.0524	0.0253	0.9989
T5	0.085	0.0309	0.9986
T6	0.1054	0.0486	0.9966
T9	0.1615	0.0762	0.9934
T11	0.1068	0.0471	0.9963
T12	0.1171	0.051	0.9977
T14	0.1223	0.0608	0.9943
T15	0.106	0.0495	0.9975
T16	0.0755	0.0345	0.9979
T17	0.1115	0.0518	0.9972
T18	0.1222	0.0536	0.9932
T19	0.1995	0.0616	0.9584
T20	0.1456	0.0699	0.9788

The graphs of maximum errors and mean errors for different patterns are plotted in Figs. 14 and 15. For these graphs, it can be concluded that the mean errors and maximum errors will expectedly decrease if the minimum correlation coefficient increase. The minimum value of correlation coefficient in the entire image is the particular area that has the worst correlation to its own target subset. As a result, the lower minimum value of correlation coefficient could make the errors larger.

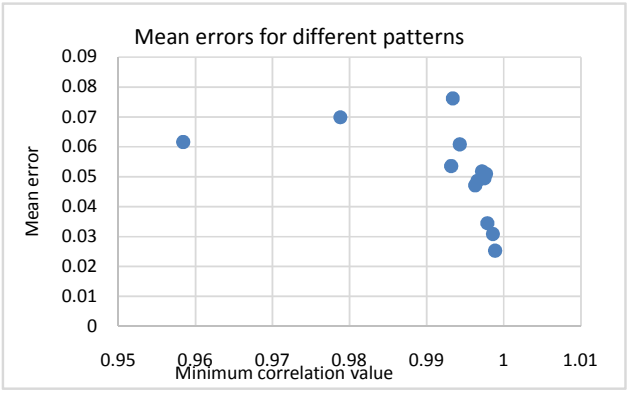

Fig. 14 Mean errors for different patterns

Fig. 15 Maximum errors for different patterns

VI. CONCLUSION

In this paper, the performance of DIC is analyzed with the quality of natural pattern in the images. The mean and maximum errors have been obtained from the experiments which depicted the performance of the DIC.

It is also analyzed that sometime DIC fails due to the small subset size used and less variation in the pattern. To avoid the failure, two methods are proposed. First is to analyze the simulation results of the patterns using that particular subset size. The other is to use ratios of maximum error over mean error to find the patterns with larger ratios which causes failure.

In this study, the effect of subset size is also analyzed. Three effects are considered including accuracy of the results, the computation time and number of iterations in optimization process. Subset size has a manifest effect on the accuracy of

the results. There is an optimum subset size which offers the lowest error. Either larger or smaller subset sizes than optimum subset size will increase the errors. Furthermore, the computation time will fluctuate for subset sizes lower than 21 x 21 pixels and it will increase significantly after subset size of 21 x 21 pixels. Also the number of iterations decreases with the increase in the subset size. It is important that the subset size is chosen in accordance with the expected error acceptance criterion. Higher accuracy comes at the cost of high computation time.

Considering the quality of natural patterns, another concept of correlation coefficient is presented. The quality of the pattern can be described by using the correlation coefficient distribution graph. The lower value of the correlation coefficient means that the corresponding area of the natural pattern is poor in quality (intensity variation). In order to assess the quality of the image, the parameter of minimum correlation coefficient is introduced. Larger minimum value of the correlation coefficient means that the quality of the pattern is better.

All the parameters having effect on the DIC are discussed and analyzed using natural patterns. Significantly for the real world application, our method to evaluate the quality of the natural patterns would be the prior work before the experiments. We could actually decide whether the quality of the image is good enough to use in the experiments before we install equipment which could save us time and cost.

REFERENCES

[1] T. C. Chu, W. F. Ranson, M. A. Sutton, and W. H. Peters, "Applications of Digital-Image-Correlation Techniques to Experimental Mechanics," *Experimental Mechanics,* vol. 25, pp. 232-244, 1985.

[2] B. Wattrisse, A. Chrysochoos, J.-M. Muracciole, and M. N. moz-Gaillard, "Analysis of Strain Localization during Tensile Tests by Digital Image Correlation," *Experimental Mechanics,* vol. 41, pp. 29-39, 2001.

[3] S. Cho, I. Chasiotis, T. A. Friedmann, and J. P. Sullivan, "Young's modulus, Poisson's ratio and failure properties of tetrahedral amorphous diamond-like carbon for MEMS devices," *J. Micromech.Microeng.,* vol. 15, pp. 728-735, 2005.

[4] S. R. McNEILL, W. H. Peters, and M. A. Sutton, "Estimation of stress intensity factor by digital image correlation," *Engineering Fracture Mechanics,* vol. 28, pp. 101-112, 1987.

[5] N. Sabaté, D. Vogel, A. Gollhardt, J. Keller, B. Michel, I. C. Cané*, et al.*, "Measurement of residual stresses in micromachined structures in a microregion," *Applied Physics Letters,* vol. 88, p. 071910, 2006.

[6] Y. Sun and J. H. L. Pang, "Experimental and numerical investigations of near-crack-tip deformation in a solder alloy," *Acta Materialia,* vol. 56, pp. 537-548, 2008.

[7] I. Gnip, S. Ve˙jelis, V. Keršulis, and S. Vaitkus, "Strength and deformability of mineral wool slabs under short-term compressive, tensile and shear loads," *Construction and Building Materials,* vol. 24, pp. 2124-2134, 2010.

[8] D. Zhang, M. Luo, and D. D. Arola, "Displacement/strain measurements using an optical microscope and digital image correlation," *Optical Engineering,* vol. 45, pp. 033605-033605-9, 2006.

[9] B. Jähne, *Practical Handbook on Image Processing for Scientific and Technical Applications*. New York: CRC Press, 2004.

[10] B. Pan, K. Qian, H. Xie, and A. Asundi, "Two-dimensional digital image correlation for in-plane displacement and strain measurement: a review," *Meas. Sci. Technol,* vol. 20, p. 062001, 2009.

[11] K. Triconnet, K. Derrien, F. Hild, and D. Baptiste, "Parameter choice for optimized digital image correlation," *Optics and Lasers in Engineering,* vol. 47, pp. 728-737, 2009.

[12] D. Lecompte, A. Smits, S. Bossuyt, H. Sol, J. Vantomme, D. V. Hemelrijck*, et al.*, "Quality assessment of speckle patterns for digital image correlation," *Optics and Lasers in Engineering,* vol. 44, pp. 1132-1145, 2006.

[13] Y. Sun and J. H. L. Pang, "Study of optimal subset size in digital image correlation of speckle pattern images," *Opt. Lasers Eng.,* vol. 45, pp. 967-974, 2007.

[14] B. Pan, H. Xie, Z. Wang, K. Qian, and Z. Wang, "Study on subset size selection in digital image correlation for speckle patterns," *Optics express,* vol. 16, pp. 7037-48, 2008.

[15] H. W. Schreier, J. R. Braasch, and M. A. Sutton, "Systematic errors in digital image correlation caused by intensity interpolation," *Opt. Eng.,* vol. 39, pp. 2915-2921, 2000.

[16] H. A. Bruck, S. R. McNeill, M. A. Sutton, and W. H. P. III, "Digital Image Correlation Using Newton-Raphson Method of Partial Differential Correction," *Experimental Mechanics,* vol. 29, pp. 261-267, 1989.

[17] S. Timoshenko and J. Goodier, *Theory of elasticity*, 2 ed.: McGraw-Hill Book Company, Inc., New York, 1951.